

# TeV $\gamma$ -rays from photo-disintegration/de-excitation of cosmic-ray nuclei

Luis A. Anchordoqui,<sup>1</sup> John F. Beacom,<sup>2</sup> Haim Goldberg,<sup>3</sup> Sergio Palomares-Ruiz,<sup>4,5</sup> and Thomas J. Weiler<sup>4</sup>

<sup>1</sup>*Department of Physics, University of Wisconsin-Milwaukee, P.O. Box 413, Milwaukee, WI 53201*

<sup>2</sup>*CCAPP, Departments of Physics and Astronomy, Ohio State University, Columbus, OH 43210*

<sup>3</sup>*Department of Physics, Northeastern University, Boston, MA 02115*

<sup>4</sup>*Department of Physics and Astronomy, Vanderbilt University, Nashville, TN 37235*

<sup>5</sup>*Institute for Particle Physics Phenomenology, University of Durham, Durham DH1 3LE, UK*

It is commonly assumed that high-energy  $\gamma$ -rays are made via either purely electromagnetic processes or the hadronic process of pion production, followed by decay. We investigate astrophysical contexts where a third process ( $A^*$ ) may dominate, namely the photo-disintegration of highly boosted nuclei followed by daughter de-excitation. Starburst regions such as Cygnus OB2 appear to be promising sites for TeV  $\gamma$ -ray emission via this mechanism. A unique feature of the  $A^*$  process is a sharp energy minimum  $\sim 10 \text{ TeV}/(\text{T/eV})$  for  $\gamma$ -ray emission from a thermal region of temperature T. We also check that a diffuse  $\gamma$ -ray component resulting from the interaction of a possible extreme-energy cosmic-ray nuclei with background radiation is well below the observed EGRET data.

**Introduction.** In the field of TeV  $\gamma$ -ray-astronomy, new instruments are discovering new sources at a rapid rate, both within our Galaxy and outside the Galaxy [1]. Not surprisingly, the brightest TeV  $\gamma$ -ray source yet discovered is the one discovered first, the Crab pulsar wind nebula. The integral  $\gamma$ -ray flux obtained from the Crab by the Whipple Collaboration is now the standard TeV flux unit:  $F_{\text{Crab}}(\epsilon_{\gamma}^{\text{LAB}} > 0.35 \text{ TeV}) = 10^{-10}/\text{cm}^2/\text{s}$  [2]. The spectral index of the Crab's integrated flux is measured to be  $-1.5$ , so  $F_{\text{Crab}}$  falls by a factor of 30 for each decade of increase in  $\min(\epsilon_{\gamma}^{\text{LAB}})$ . Newly commissioned atmospheric Cerenkov telescopes (CANGAROO, HESS, MAGIC and VERITAS) will reach a sensitivity  $\sim 100$  times below  $F_{\text{Crab}}$ .

Two well-known mechanisms for generating TeV  $\gamma$ -rays in astrophysical sources [3] are the purely electromagnetic (EM) synchrotron emission and inverse Compton scattering, and the hadronic (PION) one in which  $\gamma$ -rays originate from  $\pi^0$  production and decay. There has been considerable debate over which of these two mechanisms is dominant. The mechanism for the PION mode may be either  $pp$  or  $p\gamma$  collisions. In this Letter, we highlight a third dynamic which leads to TeV  $\gamma$ -rays: photo-disintegration of high-energy nuclei, followed by immediate photo-emission from the excited daughter nuclei. For brevity, we label the photo-nuclear process  $A + \gamma \rightarrow A'^* + X$ , followed by  $A'^* \rightarrow A' + \gamma\text{-ray}$  as " $A^*$ ". It is likely that each of the three mechanisms is operative in some environments. As we show below, the  $A^*$ -process is likely operative in the interesting complex environments which have accelerated nuclei and hot starlight. Fortunately, future measurements can readily distinguish among the three competing mechanisms per source. In particular, the nuclei of the  $A^*$  process act in analogy to a relativistically moving mirror [4], to "double-boost" eV starlight to TeV energies for a nuclear boost factor  $\Gamma_A = E_A^{\text{LAB}}/m_A > 10^6$ .

**The  $A^*$ -Process.** Nuclear photo-disintegration in the astrophysical context was first calculated by Stecker in a

seminal paper [5], almost forty years ago. To our knowledge, the possibly important role of nuclear de-excitation in the astrophysical context was first appreciated and proposed by Moskalenko and collaborators [6] more than a decade ago. Since then, the  $A^*$ -process has been overlooked by the  $\gamma$ -ray community. Now that data is becoming available which can validate or invalidate the process, it is timely to revive and further develop the  $A^*$ -process. We do so, by providing calculational details, and by identifying the astrophysical context where this process might dominate over the EM and PION modes for production of  $\gamma$ -rays. A detailed discussion on the main features of the EM and PION mechanisms is presented in a longer accompanying paper [7].

By far the largest contribution to the photo-excitation cross-section comes from the Giant Dipole Resonance (GDR) at  $\epsilon_{\gamma}^{\text{GDR}} \sim 10 \text{ MeV} - 30 \text{ MeV}$  in the nuclear rest frame [8]. The ambient photon energy required to excite the GDR is therefore  $\epsilon = \epsilon_{\gamma}^{\text{GDR}}/\Gamma_A$ . The GDR decays by the statistical emission of a single nucleon, leaving an excited daughter nucleus ( $A - 1$ )\*. The probability for emission of two (or more) nucleons is smaller by an order of magnitude. The excited daughter nuclei typically de-excite by emitting one or more photons of energies  $\epsilon_{\gamma}^{\text{dxn}} \sim 1 - 5 \text{ MeV}$  in the nuclear rest frame. The lab-frame energy of the  $\gamma$ -ray is then  $\epsilon_{\gamma}^{\text{LAB}} = \Gamma_A \epsilon_{\gamma}^{\text{dxn}}$ .

As just outlined, the boost in the nuclei energy from rest to  $E_A^{\text{LAB}} = \Gamma_A A m_N$  plays two roles. It promotes the thermal energies of the ambient photons to the tens of MeV  $\gamma$ -rays capable of exciting the GDR, and it promotes the de-excitation photons from a few MeV to much higher energies, potentially detectable in  $\gamma$ -ray telescopes. Eliminating  $\Gamma_A$  above leads to the relation  $\epsilon \epsilon_{\gamma}^{\text{LAB}} \sim \epsilon_{\gamma}^{\text{GDR}} \epsilon_{\gamma}^{\text{dxn}}$ . The " $\sim$ " indicates that the  $\epsilon_{\gamma}^{\text{GDR}}$  and  $\epsilon_{\gamma}^{\text{dxn}}$  energies are not sharp, but rather distributed over their resonant shapes ("Lorentzian" or "Breit-Wigner"). Each of the two spectra have a width to mass ratio less than unity. It is sufficient for our purposes to treat each spectrum in the narrow-width-

approximation (NWA). Well-defined values for  $\epsilon_\gamma^{\text{GDR}}$  and  $\epsilon_\gamma^{\text{dxn}}$  then result. We may *summarize up to this point by saying that the  $A^*$  process produces  $\gamma$ -ray's with energy  $\epsilon_\gamma^{\text{LAB}} = \epsilon_\gamma^{\text{GDR}} \epsilon_\gamma^{\text{dxn}} / \epsilon \sim 20 \text{ TeV}/(\text{T/eV})$  if there exists an accelerated nuclear flux with boost  $\Gamma_A \sim \epsilon_\gamma^{\text{GDR}} / \epsilon \sim 7 \times 10^6 (\text{T/eV})$  or equivalent energy  $E_A^{\text{LAB}} \sim 7 \text{ PeV}/(\text{T/eV})$  per nucleon [6, 9].*

Here (and in what follows) we have assumed a Bose-Einstein (BE) distribution with temperature  $T$  for the ambient photons; in the mean,  $\epsilon \sim 3 \text{ T}$ . As an example,  $\gamma$ -ray's with energy  $\epsilon_\gamma^{\text{LAB}} \sim 20 \text{ TeV}$  are generated in this  $A^*$ -process if an ambient photon temperature of an eV and a boost factor of  $7 \times 10^6$  are present. Thus, we have arrived at an astrophysical environment where the  $A^*$ -process may dominate production of TeV  $\gamma$ -ray's: the region must contain far-UV photons from the Lyman- $\alpha$  emission of young, massive, hot stars such as O and B stars which have surface temperatures of  $T_* \sim 40,000 \text{ K}$  (4.6 eV) and 18,000K (2.1 eV), respectively; and the region must contain shocks, giant winds, or other mechanisms which accelerate nuclei to energies in excess of a PeV per nucleon. Violent starburst regions, such as the one in the direction of Cygnus, are splendid examples of regions which contain OB stars, shocks and giant stellar winds.

With  $\epsilon_\gamma^{\text{GDR}}$  and  $\epsilon_\gamma^{\text{dxn}}$  fixed at their central values, the  $\gamma$ -ray spectrum  $dn(\epsilon_\gamma^{\text{LAB}})/d\epsilon_\gamma^{\text{LAB}}$  is given by a simple Jacobian times the BE distribution with argument  $\epsilon$  set to  $\epsilon_\gamma^{\text{GDR}} \epsilon_\gamma^{\text{dxn}} / \epsilon_\gamma^{\text{LAB}}$ , i.e.,

$$\frac{dn(\epsilon_\gamma^{\text{LAB}})}{d\epsilon_\gamma^{\text{LAB}}} \propto (\epsilon_\gamma^{\text{LAB}})^{-4} \left[ e^{(\epsilon_\gamma^{\text{GDR}} \epsilon_\gamma^{\text{dxn}} / \epsilon_\gamma^{\text{LAB}} T) - 1} \right]^{-1}. \quad (1)$$

Three regions in  $\epsilon_\gamma^{\text{LAB}}$  emerge. For  $\epsilon_\gamma^{\text{LAB}} < \epsilon_\gamma^{\text{GDR}} \epsilon_\gamma^{\text{dxn}} / T$ , the  $\gamma$ -ray spectrum is exponentially suppressed [11]. For  $\epsilon_\gamma^{\text{LAB}} \gg \epsilon_\gamma^{\text{GDR}} \epsilon_\gamma^{\text{dxn}} / T$ , there is power-law suppression. The  $\gamma$ -ray spectrum peaks near  $\epsilon_\gamma^{\text{LAB}} \sim \epsilon_\gamma^{\text{GDR}} \epsilon_\gamma^{\text{dxn}} / T$ . In particular, one notes that the suppression of the high-energy Wien end of the thermal photon spectrum has led to a similar *suppression of the photon spectrum below  $\epsilon_\gamma^{\text{LAB}} \sim 20 \text{ TeV}/(\text{T/eV})$* . This *presents a robust prediction of the  $A^*$ -process, namely a striking lower limit on the resulting  $\gamma$ -ray energy*. This lower energy limit contrasts greatly with the PION and EM processes, and so provides a unique signature. The  $A^*$  process predicts “orphan” sources, with no associated GeV  $\gamma$ -ray's or MeV X-rays (although the photo-dissociated neutrons may  $\beta$ -decay to neutrinos [10]). Observationally, orphan  $\gamma$ -ray sources have been identified [12, 13], and some orphans are known to be near OB starburst regions [14].

Comparing to the PION  $p\gamma$  process, the  $A^*$  process has a much lower ambient photon energy threshold; in the nuclear rest frame, the photon threshold is  $\epsilon_\gamma^{\text{GDR}} \sim 10 \text{ MeV}$  for the  $A^*$  process, but it is an order of magnitude larger at  $m_\pi$  for the PION  $p\gamma$  process [15]. This means that for fixed ambient temperature,  $\Gamma_A$  need be an order of

magnitude larger for the PION  $p\gamma$  process, and the resulting  $\gamma$ -ray energies, proportional to  $\Gamma_A^2$ , are two orders of magnitude larger. The EM and PION  $pp$  processes contrast with the  $A^*$ -process in that there is no threshold, and the resulting  $\gamma$ -ray spectrum rises monotonically with decreasing  $\epsilon_\gamma^{\text{LAB}}$ .

**The  $A^*$ -Rate.** We now derive the rate for  $\gamma$ -ray production in the  $A^*$ -process. The cross-section is dominated by the GDR dipole form [15], which in the NWA is

$$\sigma_A(\epsilon) \xrightarrow{\text{NWA}} \frac{\pi}{2} \sigma^{\text{GDR}} \Gamma^{\text{GDR}} \delta(\epsilon_\gamma^{\text{GDR}} - \Gamma_A \epsilon), \quad (2)$$

where  $\Gamma^{\text{GDR}}$  and  $\sigma^{\text{GDR}}$  are the GDR width and cross-section at maximum. Fitted numerical formulas are  $\sigma^{\text{GDR}} = 1.45 A \times 10^{-27} \text{ cm}^2$ ,  $\Gamma^{\text{GDR}} = 8 \text{ MeV}$ , and  $\epsilon_\gamma^{\text{GDR}} = 42.65 A^{-0.21} \text{ MeV}$  for  $A > 4$  and  $0.925 A^{2.433}$  for  $A \leq 4$  [16]. The 8 MeV width implies a very short de-excitation distance of  $\sim 25 \Gamma_A \text{ fm}$ .

The general formula for the inverse photo-disintegration mean-free-path (mfp) [17] for a highly relativistic nucleus with energy  $\Gamma_A/m_A$  propagating through an isotropic photon background with energy  $\epsilon$  and spectrum  $dn(\epsilon)/d\epsilon$  is [5, 7]

$$(\lambda_A)^{-1} \xrightarrow{\text{NWA}} \frac{\pi \sigma^{\text{GDR}} \epsilon_\gamma^{\text{GDR}} \Gamma^{\text{GDR}}}{4 \Gamma_A^2} \int_{\frac{\epsilon_\gamma^{\text{GDR}}}{2 \Gamma_A}}^{\infty} \frac{d\epsilon}{\epsilon^2} \frac{dn(\epsilon)}{d\epsilon}. \quad (3)$$

For a nucleus passing through a region of thermal photons, one easily completes the integration to find

$$(\lambda_A^{\text{BE}})^{-1} \approx \frac{\sigma^{\text{GDR}} \Gamma^{\text{GDR}}}{\epsilon_\gamma^{\text{GDR}}} \left( \frac{T^3}{\pi} \right) w^2 |\ln(1 - e^{-w})|, \quad (4)$$

where we have defined a dimensionless scaling variable  $w \equiv \epsilon_\gamma^{\text{GDR}} / 2 \Gamma_A T$ . The function  $f(w) = w^2 |\ln(1 - e^{-w})|$  is shown in Fig. 1. Approximations to the  $|\ln w|$  term yield  $e^{-w}$  for  $w > 2$ , and  $|\ln w|$  for  $w \ll 1$ . Thus, the exponential suppression of the process appears again for large for  $w > 2$ , i.e., for  $\epsilon_\gamma^{\text{LAB}} < \epsilon_\gamma^{\text{GDR}} \epsilon_\gamma^{\text{dxn}} / 4T$ , and the small  $w$  region presents a mfp that scales as  $w^2$  times a logarithm.

The peak region provides the smallest inverse mfp, and so this region dominates the  $A^*$ -process. In the peak region,  $w$  is of order one, which implies that  $\Gamma_A T \sim \epsilon_\gamma^{\text{GDR}}$ . When this latter relation between the nuclei boost and the ambient photon temperature is met, then the photo-disintegration rate is optimized.

The area under the peak region in Fig. 1 is of order one, which leads to a simple and reasonable estimate of the inverse mfp given in Eq. (4), for any nucleus boosted near  $\Gamma_A \sim \epsilon_\gamma^{\text{GDR}} / T$ . The estimate is  $(\lambda_A^{\text{BE}})^{-1} \approx \sigma^{\text{GDR}} (T^3 / 3\pi)$ ; here, we have input the typical value  $\Gamma^{\text{GDR}} / \epsilon_\gamma^{\text{GDR}} \sim 1/3$ . This result for  $\lambda^{-1}$  is useful, and eminently sensible when it is realized that  $n_\gamma^{\text{BE}} = 2\zeta(3) T^3 / \pi^2 \simeq T^3 / 4$ . Putting in numbers, this

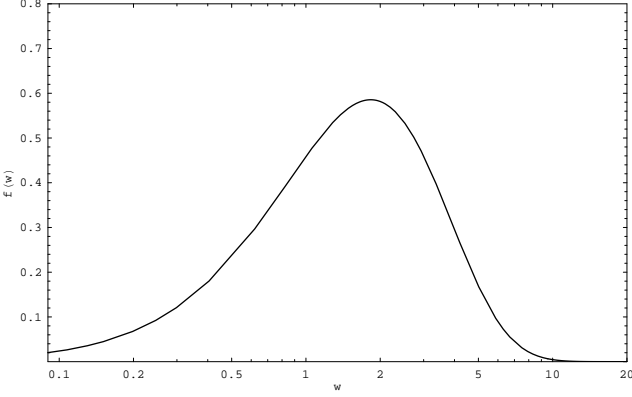


FIG. 1: The scaling function  $f(w) = w^2 |\ln(1 - e^{-w})|$ .

estimate yields

$$\lambda_A^{\text{BE}} \sim \frac{5 \times 10^{13} \text{ cm}}{A (\text{eV})^3} \sim \frac{3 \text{ AU}}{A (\text{eV})^3} \quad (5)$$

for a nucleus with energy in the peak regime around  $E_A \sim 10 A/(\text{eV}) \text{ PeV}$ .

An important question is how many photo-disintegration steps in the nuclear chain  $A \rightarrow (A-1)^* \rightarrow (A-2)^*$  etc. may be expected. Each step will produce an excited daughter which may de-excite via emission of  $\gamma$ -ray's, each having a typical lab-frame energy  $\epsilon_\gamma^{\text{LAB}} \sim \epsilon_\gamma^{\text{GDR}} \epsilon_\gamma^{\text{dxn}} / 3T$ . Clearly, the number of steps depends on the mfp of each excited daughter nucleus, and on the diffusion time of the nuclei in the thermal region. The probability for  $n$ -cascades, producing  $n$  excited daughter nuclei and  $n$  single nucleons, may be written in symmetric ways as

$$P_n = \prod_{j=1}^n \int_0^{x_{j+1}} \frac{dx_j}{\lambda_j} e^{-\frac{(x_j - x_{j-1})}{\lambda_j}} = \prod_{j=1}^n \int_0^{x_{j+1}} \frac{dx_j}{\lambda_j} e^{-x_j \delta_j}, \quad (6)$$

where  $x_0 = 0$ ,  $x_{n+1}$  equals the diffusion length  $D$  of nuclei in the  $A^*$ -region, the ordered  $x_1 \leq x_2 \dots x_n$  denote the spatial positions of successive photo-disintegrations to  $(A-1)^*$ ,  $\dots$   $(A-n)^*$ ,  $\delta_j = \lambda_j^{-1} - \lambda_{j+1}^{-1}$ , and  $\lambda_{n+1} = \infty$ . The exponentials in (6) are probabilities that the various daughters not interact (i.e., survive) from the point of creation to the point of photo-disintegration. A simple result obtains when the mfp's are long on the diffusion scale  $D$  of the  $A^*$ -region. In this case the nested integrals collapse to  $P_n \approx (n!)^{-1} \prod_{j=1}^n D/\lambda_j$ . This is just the product of the independent probabilities for each excited daughter to be produced, times the factor  $1/n!$  that divides out all but the one correct time ordering of the  $n$  photo-disintegrations. One sees that, since  $D/\lambda_j \ll 1$  by assumption, disintegration to more than the first excited daughter is unlikely. Such is the case if photo-

disintegration of nuclei occurs in the Cygnus OB starburst region, as we now demonstrate.

**Relevance to Starburst Regions.** The aforementioned possibility of generating Galactic TeV  $\gamma$ -ray's from accelerated nuclei scattering on starlight in starburst regions is of considerable astrophysical interest. The energy of the photons ( $\sim 3T_\star$  in the mean) is maintained as the photons disperse from the stars, but the photon density decreases by the ratio of the surface of stellar emission ( $N_\star \times 4\pi R_\star^2$ ) to the loss surface of the starburst region ( $4\pi R_{\text{SB}}^2$ ). Taking the giant star radius to be  $R_\star \sim 10 R_\odot$ , the radius of the starburst region to be  $R_{\text{SB}} \sim 10 \text{ pc}$ , and the stellar count to be  $N_\star \sim 2600$ , the photon density is diluted by  $\sim 10^{12}$ . According to Eq. (3),  $(\lambda_A)^{-1}$  is proportional to the photon density, and hence to this factor. Including this factor in Eq. (5), one gets the estimate  $\lambda_A \sim (56/A) (2.1 \text{ eV}/T_\star)^3 \times 10^{23} \text{ cm}$  for the nuclear mfp in the starburst region. The hot stars are dominately (95%) B type, with  $T_\star \sim 2.1 \text{ eV}$ . We note here that the diffusion time for a nucleus in the Cygnus OB starburst region is calculated to be  $\sim 10^4 \text{ yr} \sim 10^{22} \text{ cm}$ , an order of magnitude shorter than the nuclear mfp. Accordingly, one expects only a few percent of the nuclei to photo-disintegrate in the Cygnus OB region, with multiple disintegrations being rather rare.

Some early statistical-model calculations for the production of  $\gamma$ -rays through the decay of the GDR gave a mean photon multiplicity between 0.5 and 2 for the different nuclides in the chain reaction (see Ref. [7] for details). We will simplify the data by assuming that one photon is emitted per nuclear de-excitation. Then, the rate of photo-emission is just the rate of excited daughter production, which in turn is just the rate of photo-disintegration. Allowing for the  $1/r^2$  dilution of the  $\gamma$ -ray flux from the source region of volume  $V_{A^*}$  at distance  $d$ , the observed integral  $\gamma$ -ray flux  $\mathcal{F}_\gamma$  at Earth with  $\epsilon_\gamma^{\text{LAB}}$  above a few  $\text{TeV} \times (\text{eV}/\text{T})$  is then

$$\mathcal{F}_\gamma = \frac{V_{A^*}}{4\pi d^2} \frac{1}{\lambda_A^{\text{BE}}} \mathcal{F}_A, \quad (7)$$

where the flux  $\mathcal{F}_A (= c n_A)$  is integral over the energy-decade of the peak region,  $A (\text{eV}/\text{T}) \text{ PeV} < E_A < 10 A (\text{eV}/\text{T})$ . It is commonly assumed that this nuclear flux results from continuous trapping of the diffuse cosmic ray flux by diffusion in a milligauss magnetic field.

Putting into Eqs. (5) and (7) the parameters for the Cygnus OB2 region, i.e.  $R_{\text{SB}} = 10 \text{ pc}$ ,  $\lambda_A = (56/A) \times 10^{23} \text{ cm}$ , and  $d = 1.7 \text{ kpc}$ , one obtains  $\mathcal{F}_\gamma = 2 \times 10^{-10} A \mathcal{F}_A$ . Thus, an accumulated nuclear flux within Cygnus OB2 of  $f/\text{cm}^2/\text{s}$  in the PeV region gives a  $\geq \text{TeV}$   $\gamma$ -ray flux at Earth of  $\sim 10 A f \times F_{\text{Crab}} (\epsilon_\gamma^{\text{LAB}} \geq 1 \text{ TeV})$ . For example, an iron flux  $\mathcal{F}_{56} = 6 \times 10^{-5} / \text{cm}^2/\text{s}$  above a TeV leads to a  $\gamma$ -ray flux at Earth of about 3% of the Crab, just at the level measured by the HEGRA experiment for  $\gamma$ -ray's from the Cygnus OB2 direction [12]. In our accompanying paper [7] we present a more detailed

calculation of the  $A^*$ -process for this starburst region, and show that  $\mathcal{F}_{56} \sim 10^{-4}/\text{cm}^2/\text{s}$  is a credible 1% of the kinetic energy budget of Cygnus OB2.

The  $\gamma$ -ray spectral energies remain to be discussed. In the rest frame of the excited nucleus, the photon is emitted isotropically. Therefore in the lab frame, the  $\gamma$ -ray-spectrum is given by

$$\frac{dn_\gamma}{d\epsilon_\gamma^{\text{LAB}}} \propto \int d\cos\theta \delta[\epsilon_\gamma^{\text{LAB}} - \Gamma_A \epsilon_\gamma^{\text{dxn}} (1 + \cos\theta)] \\ = (\Gamma_A \epsilon_\gamma^{\text{dxn}})^{-1}, \text{ with } 1 + \cos\theta = \frac{\epsilon_\gamma^{\text{LAB}}}{\Gamma_A \epsilon_\gamma^{\text{dxn}}}. \quad (8)$$

Here,  $\theta$  is the angle between the photon and the boost direction *in the nucleus rest frame*, and so  $\epsilon_\gamma^{\text{LAB}}$  is distributed evenly between 0 and  $2\Gamma_A \epsilon_\gamma^{\text{dxn}}$  on a linear scale. Therefore, 95% of the photons have energy above  $\Gamma_A \epsilon_\gamma^{\text{dxn}}/10$ , and 99.9% above  $\Gamma_A \epsilon_\gamma^{\text{dxn}}/100$ , etc. [18]. The power spectrum and integrated power rise as  $\epsilon_\gamma^{\text{LAB}}$  and  $(\epsilon_\gamma^{\text{LAB}})^2$ , respectively, peaking somewhat sharply at  $\epsilon_\gamma^{\text{LAB}} \sim \epsilon_\gamma^{\text{GDR}} \epsilon_\gamma^{\text{dxn}}/4T \sim 10 \text{ TeV (eV/T)}$ , as explained below Eq. (4).

**The Cosmogenic  $A^*$ -Process.** One well-known application [15] of nuclear photo-disintegration occurs in the calculation of the propagation of extreme-energy cosmic nuclei in the cosmic microwave background (CMB) and cosmic infrared background (CIRB). The CMB contribution is thermal, with temperature  $T = 2.3 \times 10^{-4} \text{ eV}$ , and Eq. (5) readily yields a mfp of  $\sim A^{-1} \text{ Mpc}$  for nuclei with energies near  $E_A \sim 4A \times 10^{19} \text{ eV}$ . The CIRB, now fairly well known [19], is much smaller than the CMB. Its spectrum may be approximated by one or two power-laws, which allows an analytic integration of Eq. (3). The result is a mfp longer than that of the CMB result, but relevant to nuclei with energies down to  $10^{16} \text{ eV}$ .

Of interest in our work is the  $\gamma$ -ray flux produced when the photo-dissociated nuclear fragments produced on the CMB and CIRB de-excite. These  $\gamma$ -rays create chains of electromagnetic cascades on the CMB and CIRB, resulting in a transfer of the initial energy into the so-called EGRET region below 100 GeV, which is bounded by observation to not exceed  $\omega_{\text{cas}} \sim 2 \times 10^{-6} \text{ eV/cm}^3$  [20].

Fortunately, we can finesse the details of the calculation by arguing in analogy to work already done. Two recent papers [21, 22] have calculated the  $\bar{\nu}_e$  flux resulting from photo-disintegration of cosmic Fe, followed by  $\beta$ -decay of the associated free neutrons. The photo-disintegration chain produces one  $\beta$ -decay neutrino with energy of order 0.5 MeV in the nuclear rest frame, for each neutron produced. Multiplying this result by 2 to include photo-disintegration to protons in addition to neutrons correctly weights the number of steps in the chain. Each step produces on average one photon with energy  $\sim 3 \text{ MeV}$  in the nuclear rest frame. Comparing, about 12 times more energy is deposited into photons. Including the factor of 12 relating  $\omega_\gamma$  to  $\omega_\nu$ , we

find from Fig. 3 in Ref. [21] that cosmogenic photo-disintegration/de-excitation energy is more than three orders of magnitude below the EGRET bound [23]. This result appears to be nearly invariant with respect to varying the maximum energy of the Fe injection spectrum (with a larger  $E_{\text{max}}$ , the additional energy goes into cosmogenic pion production). Thus, there is no constraint on a heavy nuclei cosmic-ray flux from the  $A^*$  mechanism.

**Conclusion.** In final summary, we have presented an alternative mechanism ( $A^*$ ) for generating TeV  $\gamma$ -ray's in starburst regions. It has a unique orphan-like signature, with radiation absent below  $\sim 20 \text{ TeV}/(\text{T/eV})$ . This signature makes the  $A^*$  mechanism testable.

We acknowledge encouragement from V. Berezinsky, and support from NSF Grants PHY-0547102 (CAREER, JFB), PHY-0244507 (HG), NASA Grant ATP02-000-0151 (SPR and TJW), Spanish MCT Grant FPA2005-01678 (SPR), DOE grant DE-FG05-85ER40226 (TJW) and Vanderbilt University Discovery Award (TJW).

- 
- [1] Instruments and sources are reviewed by R. Ong, Rapporteur Talk at the 29th International Cosmic Ray Conference (ICRC 2005), [arXiv: astro-ph/0605191].  
[2] G. Vacanti *et al.*, *Astrophys. J.* **377**, 467 (1991); A. M. Hillas *et al.*, *Astrophys. J.* **503**, 744 (1998).  
[3] F. A. Aharonian, “Very high energy cosmic  $\gamma$  radiation: A crucial window on the extreme universe,” (Singapore, World Scientific Publishing 2004).  
[4] A. Einstein, *Annals Phys. (Leipzig)* **17**, 891 (1905).  
[5] F. W. Stecker, *Phys. Rev.* **180**, 1264 (1969).  
[6] See e.g., S. Karakula, G. Kocielek, I. V. Moskalenko and W. Tkaczyk, *Astrophys. J. Suppl.* **92**, 481 (1994); and further references in our longer companion paper.  
[7] L. A. Anchordoqui, J. F. Beacom, H. Goldberg, S. Palomares-Ruiz, and T. J. Weiler, astro-ph/0611581.  
[8] Note that we will use  $\epsilon$  for photon energies, and  $E$  for hadron and neutrino energies. It is also implicit that GDR-superscripted variables ( $\epsilon_\gamma^{\text{GDR}}$  here, and  $\Gamma^{\text{GDR}}$  and  $\sigma^{\text{GDR}}$  below) have an  $A$ -dependence.  
[9] The interesting observation that the threshold for disintegration of heavy nuclei on starlight occurs at  $\sim \text{PeV}$  and so may be related to the change of slope (the “knee”) seen in the cosmic-ray spectrum, has been noted before, in J. Candia, L. N. Epele and E. Roulet, *Astropart. Phys.* **17**, 23 (2002) [arXiv:astro-ph/0011010].  
[10] L. A. Anchordoqui, H. Goldberg, F. Halzen and T. J. Weiler, *Phys. Lett. B* **593**, 42 (2004).  
[11] This suppression characterises a mean energy. However, as explained later in the text, the differential spectrum is actually flat at low energies, so the power grows as  $E_A^{\text{LAB}}$  and the integrated power as  $E_A^{\text{LAB}}/2$ .  
[12] F. Aharonian *et al.* [HEGRA Collaboration], *Astron. Astrophys.* **431**, 197 (2005)  
[13] H. Krawczynski *et al.*, *Astrophys. J.* **601**, 151 (2004); M. K. Daniel *et al.*, *Astrophys. J.* **621**, 181 (2005); M. Blazejowski *et al.*, *Astrophys. J.* **630**, 130 (2005).

- [14] F. Aharonian *et al.* [H.E.S.S. Collaboration], *Science* **307**, 1938 (2005); F. Aharonian *et al.* [H.E.S.S. Collaboration], *Astron. Astrophys.* **439**, 1013 (2005).
- [15] F. W. Stecker and M. H. Salamon, *Astrophys. J.* **512**, 521 (1999); J. L. Puget, F. W. Stecker and J. H. Bredekamp, *Astrophys. J.* **205**, 638 (1976).
- [16] S. Karakula and W. Tkaczyk, *Astropart. Phys.* **1**, 229 (1993).
- [17]  $\lambda_A = \tau_A$  is also the mean survival time, so  $\lambda_A^{-1}$  is also the photodisintegration rate per nucleus.
- [18] Standard kinematics give the result that the half of the photons having  $\epsilon_\gamma^{\text{LAB}}$  in excess of  $\Gamma_A \epsilon_\gamma^{\text{dnn}}$  are boosted into a forward cone of half-angle  $1/\Gamma_A$ . However, we assume the nuclear flux in the  $A^*$ -region is isotropic, so the individual cones will add to give an isotropic  $\gamma$ -ray flux.
- [19] M. A. Malkan and F. W. Stecker, *Astrophys. J.* **496**, 13 (1998).
- [20] P. Sreekumar *et al.* [EGRET Collaboration], *Astrophys. J.* **494**, 523 (1998) [arXiv:astro-ph/9709257].
- [21] D. Hooper, A. Taylor and S. Sarkar, *Astropart. Phys.* **23**, 11 (2005) [arXiv:astro-ph/0407618].
- [22] M. Ave, N. Busca, A. V. Olinto, A. A. Watson and T. Yamamoto, *Astropart. Phys.* **23**, 19 (2005).
- [23]  $\omega_\nu$  is just the area under the  $E_\nu^2 dN_\nu/dE_\nu$  versus  $\ln E_\nu$  curve. We thank D. Hooper for replotting Fig. 3 in Ref. [21] for us in these units. Also from Fig. 3, one learns that the contribution to neutrino production and therefore photon production from photo-pion production is larger than via the photo-disintegration process by a factor of five for  $E_{\text{max}} = 10^{21.5}$  eV, and by fifty for  $E_{\text{max}} = 10^{22.5}$  eV.